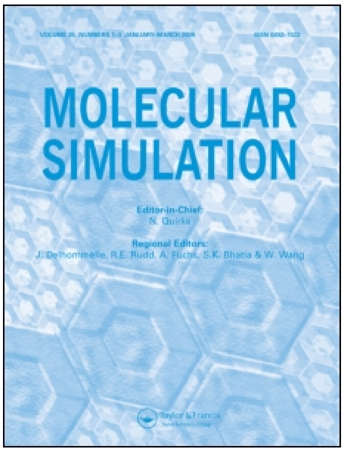

Molecular Simulation
Publication details, including instructions for authors and subscription information:
http://www.informaworld.com/smpp/title~content=t713644482

Effects of surface heterogeneity on the adsorption of nitrogen on graphitized thermal carbon black

D. D. Do[a]; H. D. Do[a]
[a] Department of Chemical Engineering, University of Queensland, St. Lucia, Qld, Australia

To cite this Article Do, D. D. and Do, H. D.(2005) 'Effects of surface heterogeneity on the adsorption of nitrogen on graphitized thermal carbon black', Molecular Simulation, 31: 9, 651 — 659

To link to this Article: DOI: 10.1080/08927020500108429

URL: http://dx.doi.org/10.1080/08927020500108429

Molecular Simulation, Vol. 31, No. 9, August 2005, 651–659

Taylor & Francis
Taylor & Francis Group

Effects of surface heterogeneity on the adsorption of nitrogen on graphitized thermal carbon black

D. D. DO* and H. D. DO

Department of Chemical Engineering, University of Queensland, St. Lucia Qld 4072, Australia

(Received November 2004; in final form January 2005)

In this paper, we study the surface heterogeneity and the surface mediation on the intermolecular potential energy for nitrogen adsorption on graphitized thermal carbon black (GTCB). The surface heterogeneity is modeled as the random distribution of "effective" carbonyl functional groups on the graphite surface. The molecular parameters and the discrete charges of this carbonyl group are taken from Jorgensen, *et al.* (*J. Am. Chem. Soc.*, (1984) **106**, 6638) while those for nitrogen (dispersive parameters and discrete charges) are taken from Murthy *et al.* (*Mol. Phys.*, (1983) **50**, 531) in our Grand Canonical Monte Carlo (GCMC) simulation. The solid surface mediation in the reduction of intermolecular potential energy between two fluid molecules was taken from a recent work by Do *et al.* (*Langmuir*, (2004) **20**, 7623). Our simulation results accounting for the surface heterogeneity and surface mediation on intermolecular potential energy were compared with the experimental data of nitrogen at 77 and 90 K. The solid-fluid dispersive parameters are determined from the Lorentz-Berthelot (LB) rule. The fraction of the graphite surface covered with carbonyl functional groups was then derived from the consideration of the Henry constant, and for the data of Kruk *et al.* (*Langmuir*, (1999) **15**, 1435) we have found that 1% of their GTCB surface is covered with "effective" carbonyl functional groups. The damping constant, due to surface mediation, was determined from the consideration of the portion of the adsorption isotherm where the first layer is being completed, and it was found to take a value of 0.0075. With these parameters, we have found that the GCMC simulation results describe the data over the complete range of pressure substantially better than any other MC models in the literature. The implication of this work is demonstrated with local adsorption isotherms of 10 and 20 A slit pores. One was obtained without allowance for surface mediation, while the other correctly accounts for these factors. The two local isotherms differ substantially, and the implication is that if we used incorrect local isotherms (i.e. without the surface mediation) the pore size distribution would be incorrectly derived.

Keywords: Adsorption; Carbon black; Slit pores; Nitrogen; Surface heterogeneity; Surface mediation

1. Introduction

Physical characterization of surfaces and porous media for surface area, pore volume and pore size has been routinely carried out with nitrogen adsorption at its boiling point (77.35 K). Analysis of the data for the required properties has been traditionally done with classical theories, such as the BET method [5] for surface area, the BJH [6] for mesopores and the HK method [7] for micropores. These methods as well as their many variants are very simplistic and contain some unrealistic assumptions, and recently they have been replaced by advanced molecular simulation methods, Monte Carlo (MC) simulation, Molecular Dynamics and Density Functional theories. With the availability of high speed computer, the applications of these modern tools are now widely accepted. Among the many MC simulation methods, the Grand Canonical Monte Carlo (GCMC) [8,9] is often used in adsorption [10–12] because of its specification of volume, temperature and chemical potential, which mimics the adsorption into an open pore system. This tool can be applied to analyze adsorption on surfaces. However, straightforward applying the GCMC to simulate this problem yields reasonable description of the isotherm, except in the region where the first layer is being completed. The GCMC simulated results over-predict the experimental data in this region [3], where molecules are getting closer to each other. What this implies is that the over-prediction in the adsorption isotherm is due to the over-estimation of the fluid–fluid interaction. When two fluid particles are close to the surface, the interaction energy, if calculated using the same equation as that for the bulk phase, is greater than what it should be. It is the surface mediation that reduces the fluid–fluid interaction,

---

*Corresponding author. Tel: +61-7-3365-4154. Fax: +61-7-3365-2789. E-mail: duongd@cheque.uq.edu.au

Molecular Simulation
ISSN 0892-7022 print/ISSN 1029-0435 online
http://www.tandf.co.uk/journals
DOI: 10.1080/08927020500108429

and the degree of this reduction depends on how close the particles are toward the surface. In other words, this reduction degree varies with the strength of solid–fluid interactions of the two particles.

Instead of arguing the surface mediation as we have just discussed above, the over-prediction of the GCMC-simulation results over the experimental data could be attributed to the surface heterogeneity. This argument lacks credibility as only homogeneous surface could give rise to sharp transition at low temperatures and there are abundant evidence in the literature that adsorption of many species on graphitized thermal carbon black (GTCB) does give rise to a clear first-order transition. Furthermore, the homogeneity of the surface can also be detected in the isotherm at low pressure, presented as the logarithm of amount adsorbed vs. the logarithm of pressure, where a slope of unity is always observed for GTCB. Thus, we argue that the surface mediation is the reason for the over-prediction of the GCMC results if that effect is ignored. This surface mediation has been raised and discussed in some papers in the literature, for example, Sinanoglu and Pitzer [13] and Everett [14]. One fundamental physical reason for the reduction of the intermolecular potential energy was provided by McLachlan [15]. When two particles are close to the surface, they create dipole images across the graphite surface. The image dipole of one particle repulses the dipole of the other particle and vice versa. Hence, the net result is the reduction in the potential energy among the two particles. However, these analyses are not easily applied to adsorption problem, and we have presented in this paper a simpler, but effective, equation to account for this surface mediation [3]. We will discuss this in more details in the next section.

In this paper, we will address the adsorption of nitrogen on GTCB. This material is not perfectly homogeneous, but is well known for its high degree of homogeneity. It does contain a small amount of functional groups on the surface, and it can affect the slope of the adsorption isotherm (i.e. Henry constant). Various authors, such as Laine *et al.* [16] have reported that the fraction of surfaces covered with functional groups is in the range of 0.5–1.5% for this highly homogeneous surface. We will assume a model for this GTCB, and determine the fraction of the functional group so that the GCMC-Henry constant agree with the experimental value. Because, nitrogen is very popular in its use in almost every characterization of surfaces or porous media, there are many studies that can be found in the literature for this topic. Among the many studies of nitrogen on carbon black and in slit pores, Brodskaya and Piotrovskaya [17,18] have compared the differences between the quasi-spherical model and dumbbell model for nitrogen adsorption in slit pores. They did not consider the quadrupole moments of nitrogen, which is important in the case where the surface contains some functional groups. Bottani and Bakaev [19] accounted for the quadrupole for nitrogen adsorption in slit pores and they used the potential model suggested by Murthy *et al.* [2]. Details of this model will be presented later. Similarly, Cracknell *et al.* [20] also studied the quadrupole effect in slits and instead of three discrete charges used in the Murthy model they proposed a model with a set of four discrete charges, which consumes more computational time than the Murthy *et al.*'s model. These authors presented simulation results without any reference to experimental data. Recently, Potoff and Siepmann [21] proposed a TraPPE model for nitrogen, which in essence similar to the model of Murthy *et al.* but their molecular parameters were obtained by matching the simulation results against the VLE data. In this paper, we will study the Murthy *et al.*'s model in the description of nitrogen adsorption on GTCB, and apply the equation to account for the surface mediation suggested in our earlier work [3] to determine the concentration of the functional group.

2. Theory

Our present MC analysis of nitrogen adsorption on GTCB involves two key points. One is the surface mediation on the fluid–fluid interaction and the other is the presence of functional groups on the graphite surface. The Grand Canonical Ensemble, first introduced by Norman and Filinov [9] and later by Adams [8] is used in the MC simulation. Details of this method can be found in Frenkel and Smit [22]. We only briefly give here the parameters that we employed in our simulation. For simulation of adsorption on a surface, we use a slit pore having a width of 80 A, which is practically large enough to simulate two independent surfaces. The box length is 10 times the collision diameter, and the cut-off radius is half of the box length. We use 50,000 cycles for equilibration, and the same number for statistic collection. In each cycle, we have N displacements and rotations, where N is the number of particles in the box, and the number of insertion or deletion is such that the successful attempt is 2% of the acceptance ratio.

2.1. Two dispersive-site potential model

The potential model for nitrogen contains two interactive dispersive sites and a set of discrete charges lying on the molecular axis joining the two centers of nitrogen atoms. We denote i and j for the two particles, and a and b for the two sites on each particle. Assuming the interaction between two sites is described by the Lennard-Jones (LJ) 12–6 equation, we can write the interaction energy between the site a on molecule i and the site b on molecule j as:

$$\varphi_{i,j}^{(a,b)} = 4\varepsilon^{(a,b)}\left[\left(\frac{\sigma^{(a,b)}}{r_{i,j}^{(a,b)}}\right)^{12} - \left(\frac{\sigma^{(a,b)}}{r_{i,j}^{(a,b)}}\right)^{6}\right] \tag{1}$$

Here, we reserve the subscript for particle and the upper-script for site. Knowing the site–site interaction, the interaction between two molecules is simply the summation of all M dispersive sites. Nitrogen has a quadrupole moments ($-4.9 \times 10^{-40}\,\mathrm{cm}^{-2}$) as well as higher moments. This is accounted for specifying a set of discrete charges and their locations along the molecular axis. Hence, beside the dispersive interaction that we have just described in the above paragraph, the set of discrete charges results in electrostatic interaction between two particles. The electrostatic interaction energy between a charge α on a molecule i and a charge β on a molecule j is determined via the Coulomb law of electrostatic interaction [23]. In the MC simulation of adsorption in a slit pore, the electrostatic interaction between a selected particle (whether it be a randomly selected particle in the translational–rotational move or a newly created particle in the insertion move) and all other particles is required [24].

Let us now discuss the various potential models that have been proposed for nitrogen in the literature. The simplest model that involves a set of three charges is that of Murthy *et al.* [2] (hereafter, we denote as MOM model). It involves two dispersive sites, whose locations are on the centers of nitrogen atoms, and three charges lying along the molecular axis joining the two centers. One positive charge (0.810e) is at the center of the molecular axis and the two symmetric negative charge (−0.405e) are on the same axis with a distance of 1.1 A from each other. The collision diameter and the well-depth of interaction energy of the nitrogen atom are $\sigma^{\mathrm{N-N}} = 3.32\,\mathrm{A}$, $\varepsilon^{\mathrm{N-N}}/k = 36.4\,\mathrm{K}$. The distance between the two LJ sites is the same as that between two negative charges. Another model for nitrogen is suggested by Cracknell *et al.* [20] (hereafter, we denote as CNTB). This model involves two dispersive sites and a set of four charges, and like the MOM model these charges lie on the molecular axis. These four charges lie symmetrically with respect to the molecular center of mass. The distance between two positive charges of 0.373e is 1.694 A, while that between two negative charges of −0.373e is 2.088 A. The distance between two LJ sites is 1.094 A and the collision diameter and the well-depth of the interaction energy are $\sigma^{\mathrm{N-N}} = 3.318\,\mathrm{A}$; $\varepsilon^{\mathrm{N-N}}/k = 37.8\,\mathrm{K}$. Many authors have studied adsorption of nitrogen and modeled it as a quasi-spherical model, for example, Maddox *et al.* [25] suggested $\sigma = 3.75\,\mathrm{A}$ and $\varepsilon/k = 95.2\,\mathrm{K}$ while Neimark and Vishnyakov [26] proposed $\sigma = 3.6154\,\mathrm{A}$ and $\varepsilon/k = 101.5\,\mathrm{K}$. Since, these models do not explicitly account for charges, they are not suitable in the investigation of the interaction of nitrogen with surfaces containing functional group. Therefore, they are not considered here.

2.2. *Solid–Fluid potential*

The interaction potential energy between a site a of the molecule i and the homogeneous flat solid substrate is calculated by the 10–4–3 Steele potential [27,28]. It takes the following form:

$$\varphi^{(a)}_{i,s} = 4\pi\rho_C\varepsilon^{(a,s)}\left[\sigma^{(a,s)}\right]^2\Delta\left\{\frac{1}{5}\left(\frac{\sigma^{(a,s)}}{z^a_i}\right)^{10} - \frac{1}{2}\left(\frac{\sigma^{(a,s)}}{z^a_i}\right)^{4} - \frac{\left[\sigma^{(a,s)}\right]^4}{6\Delta\left(0.61\Delta + z^a_i\right)^3}\right\} \tag{2}$$

The solid–fluid molecular parameters, the collision diameter $\sigma^{(a,s)}$ and the interaction energy $\varepsilon^{(a,s)}$, are calculated from the usual Lorentz-Berthelot (LB) mixing rule. The solid–fluid interaction energy of the molecule i is $\varphi_{i,s} = \sum_{a=1}^{M}\varphi^{(a)}_{i,s}$ and the potential energy between one molecule with a pore of slit shape and width H is $\varphi_{i,p} = \varphi_{i,s}(z) + \varphi_{i,s}(H-z)$. Here, the pore width H is defined as the distance between one plane passing through all carbon atoms of the outermost layer of one wall to the corresponding plane of the other wall.

2.3. *Surface heterogeneity*

As we have mentioned in the introduction section, even the GTCB contains some groups of atoms (other than carbon atoms of the basal graphite layer). These functional groups, despite their low concentration, can impart on the behavior of the Henry constant. In this sub-section, we will discuss the modeling of functional group. We introduce this chemical heterogeneity by allowing a random distribution of functional groups on the surface. There are various functional groups that have been identified for carbon surface. Here, we shall choose the carbonyl group C═O (as a representative) with its carbon grafted in the outermost graphite surface. The oxygen atom basically sits on the outermost surface of graphite as shown in figure 1 (white particle). The molecular parameters of this oxygen atom are $\sigma^{(\mathrm{O,O})} = 2.96\,\mathrm{A}$ and $\varepsilon^{(\mathrm{O,O})}/k = 105.8\,\mathrm{K}^1$. Since, the carbon and oxygen atoms of this carbonyl group have different electro-negativity, this is modeled by assigning discrete charges on these atoms. The charge on the carbon atom is 0.5e and that on the oxygen atom is −0.5e, and the distance between the two charges is 1.233 A.

The potential energy of interaction between the adsorbate molecule and the oxygen atom is calculated from the classical LJ 12–6 potential equation. LB mixing rules are used to calculate the cross molecular parameters, and the minimum image convention is applied for this calculation of this dispersive interaction. No long range

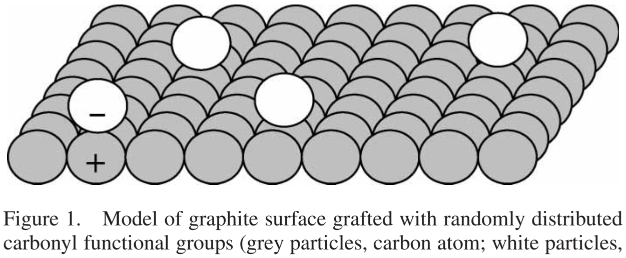

Figure 1. Model of graphite surface grafted with randomly distributed carbonyl functional groups (grey particles, carbon atom; white particles, oxygen atom).

correction is applied and since the cut off radius is typically 5 times the collision diameter, the ignorance of the long range correction for the short ranged dispersive force is justified. On the other hand, the electrostatic interaction between charges on the nitrogen molecule and those on the carbonyl functional groups is calculated from the Coulomb law, and the long range correction introduced by Heyes and van Swol [24] is used because of the slowly decaying property of the electrostatic interaction.

The graphite surface has a theoretical density of 0.382 carbon sites per 1 A^2. Let λ be the percentage of this surface is covered with carbonyl functional group. Thus, the number of functional group per 1 A^2 is 0.382 $\lambda/100$. If the graphite layer of the simulation box has lengths of L_x and L_y along the x and y directions, respectively, the total number of carbonyl functional group is $2L_xL_y(0.382(\lambda/100))$. The factor 2 in this equation accounts for two surfaces in a slit pore. These functional groups are then randomly distributed on the two graphite surfaces. This random positioning of these functional groups is subject to a constraint that not any two sites are closer than a threshold distance. In this paper, we choose a threshold distance of 4 A.

2.4. *Surface mediation*

The intermolecular potential energy between two sites, each of which on different particles, in the bulk fluid (no external force) is described by the LJ 12–6 potential energy equation (equation 1). When these two sites are close to a surface, the interaction of the solid surface on these sites, more or less, modifies the inherent properties of the two sites (polarization by the electric field emanating from the graphite layer) in such a way that the effective intermolecular potential energy is less than that if they were in the bulk. We propose that this effective intermolecular potential energy between the site a of the molecule i and the site b of the molecule j is calculated from [3]:

$$\left[\varphi_{i,j}^{(a,b)}\right]^{\text{eff}} = g\left(\varphi_{i,s}^{(a)}, \varphi_{j,s}^{(b)}\right)\varphi_{i,j}^{(a,b)} \tag{3a}$$

where $\varphi_{i,j}^{(a,b)}$ is calculated from the LJ 12–6 equation (equation 1), $\varphi_{i,s}^{(a)}$ is the solid–fluid interaction energy of site a on particle i and $\varphi_{j,s}^{(b)}$ is that of site b on particle j (equation 2). The function $g\left(\varphi_{i,s}^{(a)}, \varphi_{j,s}^{(b)}\right)$ is called the surface induced damping factor. A functional form of this factor was proposed by Do *et al.* [3], but in this paper we suggest the following simpler equation

$$g\left(\varphi_{i,s}^{(a)}, \varphi_{j,s}^{(b)}\right) = \exp\left\{-\chi\left|\varphi_{ij,s}^{(a,b)}\right|/kT\right\} \tag{3b}$$

where $\varphi_{ij,s}^{(a,b)}$ is a geometric average between $\varphi_{i,s}^{(a)}$ and $\varphi_{i,s}^{(b)}$. In this empirical equation, the damping parameter χ represents how fast the damping factor decreases with the solid–fluid interaction energy. We shall investigate this damping constant as a function of temperature.

As mentioned in the introduction, the surface mediation was considered by a number of workers. Kim and Steele [30] have considered this solid surface mediated reduction in the intermolecular potential energy in an empirical way, in which they proposed that whenever both molecules are in the first layer their interaction will follow the same equation as that in the bulk but the molecular parameters are different from those used in the bulk phase. For methane adsorption on graphite they have found that the well depth of the 2D layer is decreased by 8% while the collision diameter of the 2D layer is increased by 0.02 A. Instead of doing this, we proposed a reduction function and the reduction is greatest when two particles are in the first layer, but the reduction is lesser gradually when the particles are away from the first layer. This reduction has been found to depend directly on the polarization [3] for the case of noble gas family.

2.5. *Isosteric heat*

The isosteric heat can be obtained directly from the simulation. It has the following form [31]:

$$q_{\text{iso}} = \frac{\langle U\rangle\langle N\rangle - \langle UN\rangle}{\langle N^2\rangle - \langle N\rangle\langle N\rangle} + kT \tag{4}$$

where $\langle\rangle$ is the ensemble average and U is the configuration energy of the system. Implicit in this equation [32] are (i) ideal gas behavior of the vapor phase, (ii) the kinetic energy of the adsorbed phase is the same as that of the vapor phase, (iii) the volume of the adsorbed phase is negligible and (iv) the intra-molecular potential energy is unchanged from vapor phase to adsorbed phase.

3. Results and discussion

From the GCMC simulation of slit pore of 80 A to simulate the two independent of graphite surface, the following variables can be obtained: (i) the ensemble average number of particle $\langle N\rangle$, (ii) the isosteric heat and subsequently (iii) the average surface excess vs. pressure, (iv) the local density distribution vs. distance z from the surface and (v) the 3D-orientation-dependent local density vs. distance z and the angle θ formed between the molecular axis and the z-direction. The average surface excess is defined as

$$\Gamma_{\text{av}} = \frac{\langle N\rangle}{L_xL_y} - \frac{\rho\left[L_xL_y(H - \sigma_{ss})\right]}{L_xL_y} \tag{5}$$

where ρ is the bulk molecular density, L_x and L_y are the box lengths in the x and y-directions, respectively. The local density at a distance z from the surface is defined as:

$$\rho(z) = \frac{\langle\Delta N(z)\rangle}{L_xL_y\Delta z} \tag{6}$$

where $\Delta N(z)$ is the number of molecules whose centers of mass are in the segment whose boundaries are at z

and $z + \Delta z$. The 3D orientation-dependent local density is calculated from [33]

$$\rho(z, \theta) = \frac{\langle \Delta N(z, \theta) \rangle}{L_x L_y \Delta z \sin\theta \, \Delta\theta} \quad (7)$$

where $\Delta N(z,\theta)$ is the number of nitrogen molecules whose centers of mass are in the segment having boundaries z, $z + \Delta$ and the angle between the axis of the molecule and the z direction falls between θ and $\theta + \Delta\theta$. The 3D-orientation dependent density plot allows us to evaluate the preferential orientation of the molecules located at various distances from the surface. An angle of 0 means that the molecule lies perpendicular to the pore wall, while a value of $\pi/2$ indicates that the molecule is parallel to the pore surface.

3.1. Graphitized thermal carbon black

Extensive data of nitrogen adsorption on GTCB at 77 K are available from Isirikyan and Kiselev [33] and Kruk *et al.* [4]. Limited data at higher temperature, 90 K, is available from Ross and Winkler [34]. We first analyze the 77 K data, using the MOM model. It should be noted that we calculate all cross parameters from the LB mixing rule (that is we do not need to introduce the binary interaction parameter). The only adjusting parameters in our work are the percentage of graphite surface is covered with "effective" carbonyl group and the damping constant (λ), for the surface mediation (χ). In the very low pressure region where the adsorbed molecules are far apart, the surface mediation is insignificant and hence the data in the low pressure region can be used to determine the fraction of surface that is covered with carbonyl functional group. When the first layer is being completed, the adsorbate–adsorbate interaction is becoming significant; thus, we can use some data (here, we use only one data point) in this region to determine the damping constant, χ.

Using the low pressure data (or the Henry constant), we compare the experimental results with the GCMC-simulated data and found that a fraction of 1% of the surface is covered with the functional group. This falls within the range reported in the literature of active surface area by using chemisorption study [16,36]. For example, Graham [36] reported that the fraction of active sites (contributed by functional groups) varies from 0.1 to 1.25% of the total surface and Laine *et al.* [16] reported a range of 0.24–1.25%.

Let us first simulate the adsorption isotherm with no allowance for the surface mediation, i.e. $\chi = 0$. The GCMC simulation results for adsorption isotherm (solid lines) are shown in figure 2 in both log–log scale (to highlight the low pressure region) and linear scale (to highlight the high pressure region). We see that the simulation isotherm does not describe correctly the experimental isotherm behavior in the region of completion of the first layer (pressures between 5 and 50 Pa; see figure 2a), and this has propagation effects to the second and higher layers (figure 2b). This indeed emphasizes the importance of the surface mediation.

Let us turn to the situation where we allow for surface mediation. Once we have found the fraction of surface covered with functional group using the low pressure data where the fluid–fluid interaction is negligible, we turn to using one data point in the region of monolayer formation to determine the damping constant. Here, we choose the pressure of 20 Pa, at which approximately 50% of the surface is covered with nitrogen molecules. To match the GCMC result with the data at 20 Pa, we found that the damping constant takes a value of 0.0075, compared to 0.02 reported earlier by Do *et al.* [3], where we did not account for surface functional group and the set of discrete charges on nitrogen molecule. In that work, to reproduce the Henry constant we have to introduce the binary interaction parameter into the LB rule to calculate the well-depth for the solid–fluid interaction and found that this value was −0.04. A negative value of the binary interaction parameter obtained in our earlier work means that the surface interacts stronger than that predicted purely by the LB rule. One possible explanation for this stronger solid–fluid interaction is the presence of the functional group, and this is the focus of this paper.

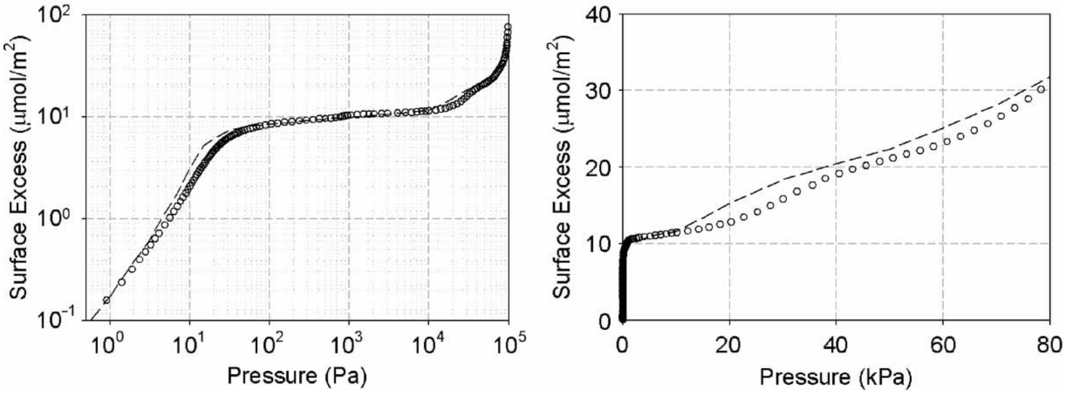

Figure 2. Adsorption isotherm of nitrogen on GTCB at 77 K for the case of no surface mediation (a) log–log scale; (b) linear scale (circle symbols, experimental data; dashed line, GCMC simulation results without surface mediation).

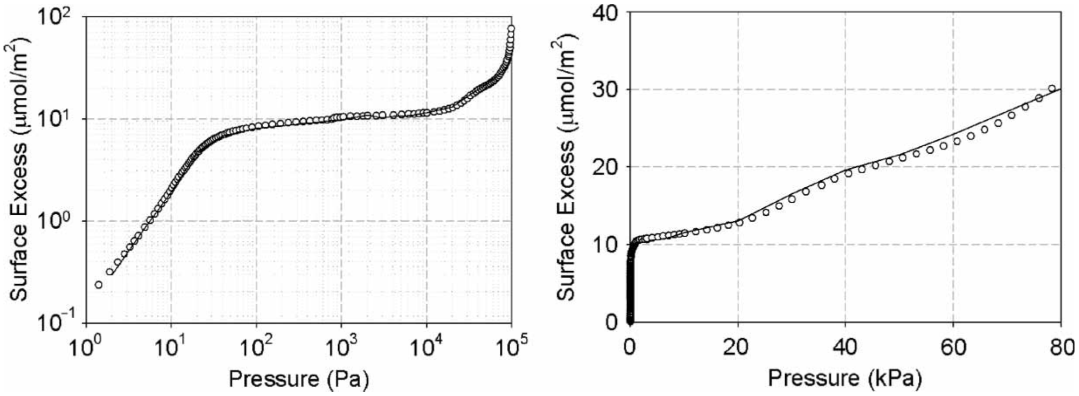

Figure 3. Adsorption isotherm of nitrogen on graphitized thermal carbon black at 77 K for the case of surface mediation (a) log–log scale; (b) linear scale (circle symbols, experimental data; solid line, GCMC simulation results with surface mediation).

Having the required two parameters, $\lambda = 1$ (1% of surface covered with functional groups) and $\chi = 0.0075$ for the damping constant, we simulate the adsorption isotherm at 77 K and the results are shown in figure 3 as plot of the surface excess vs. pressure, with figure 3a showing the plot in logarithm scale to highlight the low pressure region and figure 3b in linear scale to emphasize the high pressure region. The experimental data of Kruk *et al.* [4] are also shown in the same figure (circle symbols), and it is seen that the agreement is excellent, supporting the presence of small functional group and the solid mediation of the fluid–fluid interaction.

3.1.1. One-layer coverage

Having the good agreement between the new model for nitrogen and surface in terms of adsorbed concentration vs. pressure, we now study the orientation of nitrogen molecules in terms of the loading on the surface. First, we investigate this when 50% of the surface is covered with nitrogen molecules (at which the pressure is about 20 Pa). At this pressure, only one peak is observed at about 3.3 A from the pore surface and this corresponds to the first layer of adsorption as shown in the local density distribution plot vs. distance in figure 4a. The orientation of nitrogen molecules in this layer is dominantly parallel to the surface as shown in the plot of the 3D-local density distribution as a function of distance from the pore surface and the angle between the molecular axis and the z-axis (figure 4b), but we also note that there are some populations of nitrogen molecules that have orientations different from the parallel orientation.

The dominant parallel orientation can be investigated for the alignment of nitrogen molecules in this contact layer, and this is shown in figure 5, the snap shot of nitrogen alignment in the contact layer. In this figure, it is seen that the alignment of most nitrogen molecules is such that they form an angle of $\pi/2$ with each other. This is the energetically favorable position.

3.1.2. Two-layer coverage

Next, we would like to investigate whether the parallel orientation of nitrogen observed when only one layer has been formed on the surface will change when there are two layers on the surface because of the possibility of the interaction between nitrogen molecules in the second layer and those in the contact layer. Consider $P = 40,000$ Pa, at which we have two layers of nitrogen molecule on top of the surface. This is shown in the local density plot of figure 6a and the 3D-orientation dependent density plot in figure 6b. The orientation of molecules in the contact (first) layer is remained mostly parallel to the surface; however, we observe that the fraction of molecules having a vertical orientation in this layer is greater than that when we have only one layer on the surface (cf. figure 4), and this is due to the fluid–fluid interaction between molecules in the first

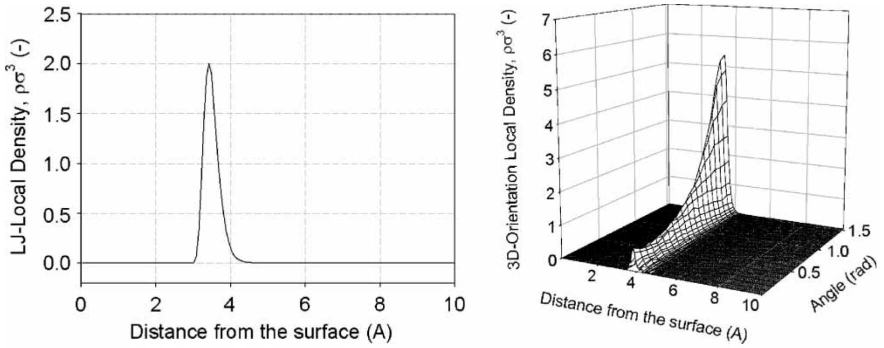

Figure 4. Local density distribution for $P = 20$ Pa (a) 2D plot of density vs. distance, (b) 3D plot of density vs. distance and angle formed between the molecular axis and the z-axis. The local density is expressed in non-dimensional quantity, $\rho\sigma^3$.

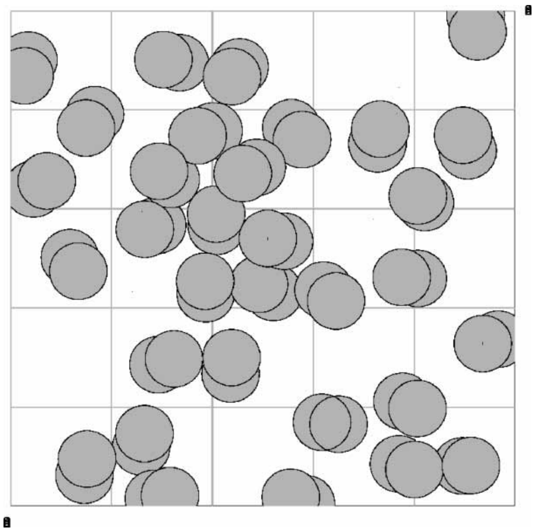

Figure 5. Snap shot of nitrogen molecules in the contact layer at 20 Pa.

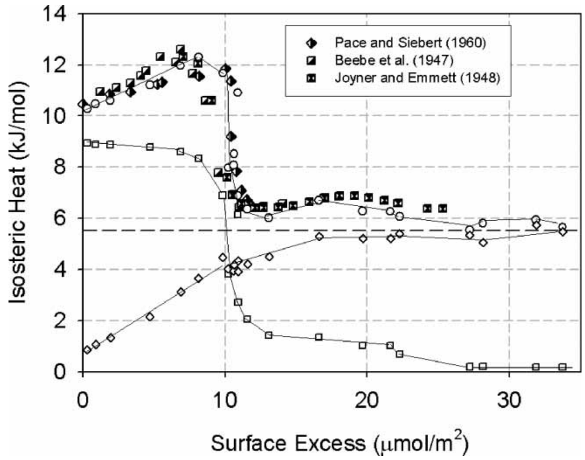

Figure 7. Isosteric heat of nitrogen vs. loading at 77 K (unfilled circle symbols, isosteric heat from GCMC simulation; unfilled square symbols, contribution from solid–fluid interaction; unfilled triangle symbols, contribution from fluid–fluid interaction).

and second layers. The orientation of molecules in the second layer exhibits no preference as the fluid–fluid interaction is more important in this second layer than the solid–fluid interaction.

3.1.3. Isosteric heat. The potential model for nitrogen can be further tested with its performance in the description of the experimental isosteric heat vs. loading. We show in figure 7, the plot of the isosteric heat of nitrogen on GTCB vs. loading for 77 K. Data on heat of adsorption are available in the literature, for example, Beebe *et al.* [36], Joyner and Emmett [37], Graham [35], Pace and Siebert [38], Isirikyan and Kiselev [33] and Piper *et al.* [39]. Some of these data have been used in figure 7 as half-filled symbols. As seen in this figure, within the scatter of various sources of data, the model describes reasonably well the behavior of the isosteric heat vs. loading.

Also plotted in figure 7 are the isosteric heat contributed by the solid–fluid interaction (unfilled square symbols) and that contributed by the fluid–fluid interaction (unfilled triangle symbols). Within the region of the contact layer (loading is less than 10 μmol/m^2), the heat contributed by the solid–fluid interaction exhibits a small decline with loading (solid line with open square symbols). This is due to the small increase in the number of nitrogen molecules that adopt the vertical orientation. Once the first layer is completed and the second layer is started, the heat by solid–fluid interaction decreases very sharply and this is simply due to molecules in the second layer are now a further distance away from the surface. For the heat contributed by the fluid–fluid interaction, it increases linearly in the region of monolayer coverage, and this rate of increase is decreased for higher loadings. In the limiting case of very high loading, the isosteric heat is dominantly contributed by the fluid–fluid interaction and it should approach the heat of liquefaction. This is indeed the case as we see in figure 7 that when the loading is above 30 μmol/m^2 (three adsorbed layers) the isosteric heat is approximately equal to the heat of liquefaction (shown as horizontal dashed line). What that means is that molecules in the third and higher layers behave very much like liquid phase. The compression due to the solid–fluid interaction occurs only in the first layer and to some extent in the second layer.

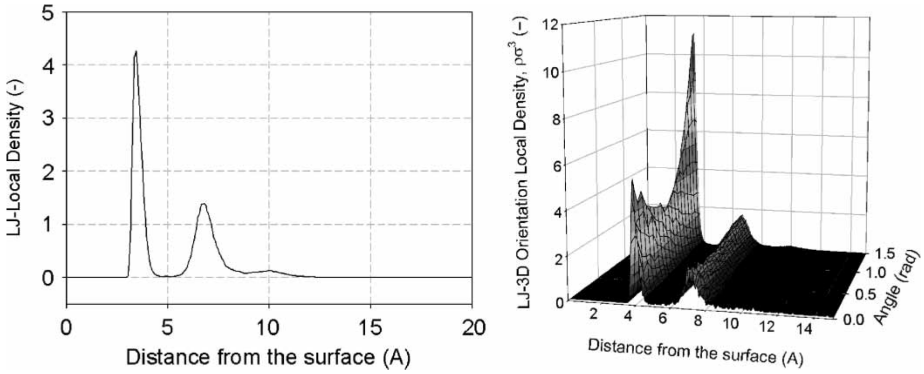

Figure 6. Local density distribution for $P = 40,000$ Pa (a) 2D plot of density vs. distance, (b) 3D plot of density vs. distance and angle formed between the molecular axis and the z-axis. The local density is expressed in non-dimensional quantity, $\rho\sigma^3$.

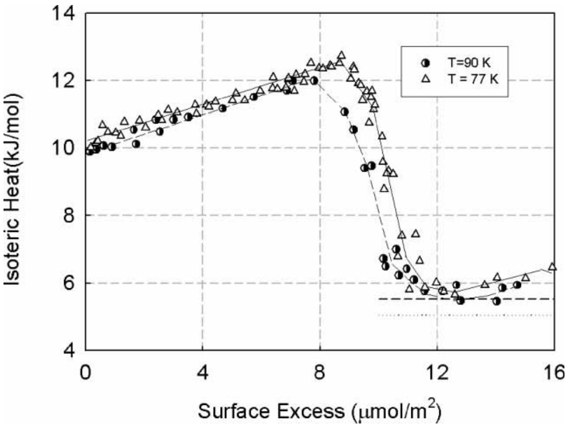

Figure 8. GCMC-simulated isosteric heat vs. loading (triangle symbols, 77 K; half-filled circle, 90 K; horizontal dashed line, heat of vaporization at 77 K; horizontal dotted line, heat of vaporization at 90 K).

3.1.4. 90 K data. Next, we consider the nitrogen adsorption data of Ross and Winkler [34] at 90 K. Following the same procedure as we did for the case of 77 K earlier, we found that the surface coverage is 0.5%, which is less than that obtained for 77 K with the GTCB used by Kruk *et al.* [4]. The difference is most likely due to the different degree of heterogeneity of the two samples used by Ross and Winkler [34] and Kruk *et al.* [4]. Nevertheless, the small value of surface coverage with functional group indicates the high degree of homogeneity of these samples of GTCB. The damping constant for 90 K was found to be 0.0055, which is again smaller than that in the case of 77 K (0.0075). One possible reason is that at high temperatures, the vibration and rotation of molecules is greater, making the distortion of electrons unlikely; hence the surface effect on the fluid–fluid interaction is less significant.

In figure 8, we show the GCMC-simulated isosteric heat vs. loading for the case of 77 and 90 K.

We see that the 77 K isosteric heat is slightly more structure than the 90 K case, and this is due to the better molecular arrangement of nitrogen molecules at lower temperatures. Furthermore, the isosteric heat at zero loading is different for different temperatures (lower for higher temperature), and the rate of increase of the heat of adsorption with loading is the same for both temperatures, suggesting the somewhat similar molecular arrangement in the monolayer coverage, and to some extent this is also observed with the second layer. Finally, the heat of adsorption approaches the heat of liquefaction at high loadings and this is indeed observed for both temperatures. The heat of liquefactions at 77 and 90 K are 5.53 (dashed line) and 5.06 kJ/mol (dotted line), respectively.

3.2. *Slit pores*

In this section, we show as a typical example how the surface mediation affects the adsorption isotherms in slit pore. We take 10 and 20 A slit pores to illustrate our point. Figure 9 shows the adsorption isotherms in these pores for the case of no surface mediation (half-filled symbols) and for the case with surface mediation (unfilled symbols). In the case of 10 A pore in which two molecular layers can be accommodated, we have a 2D condensation and this occurs at a pressure of 0.5 Pa for the case of surface mediation and at a pressure of 0.3 Pa for the case of no surface mediation. Similarly, in the case of 20 A pore we have a molecular layering mechanism followed by a pore filling. The latter occurs at 9000 Pa for the case of surface mediation and at 7000 Pa for the case of no surface mediation. These condensation pressures affect significantly in the determination of pore size; thus if the incorrect local isotherms (obtained without surface mediation) are used in the determination of pore size distribution, the result might not be very reliable.

4. Conclusions

We have presented in this paper an analysis of adsorption of nitrogen on GTCB by accounting for the presence of functional group on the surface and the effects of surface mediation on the fluid–fluid interaction energy. Nitrogen is modeled as a linear particle with two dispersive sites and a set of three charges along the molecular axis, and the functional group is modeled as “effective” carbonyl group. Analyzing the experimental data of Kruk *et al.* at 77 K,

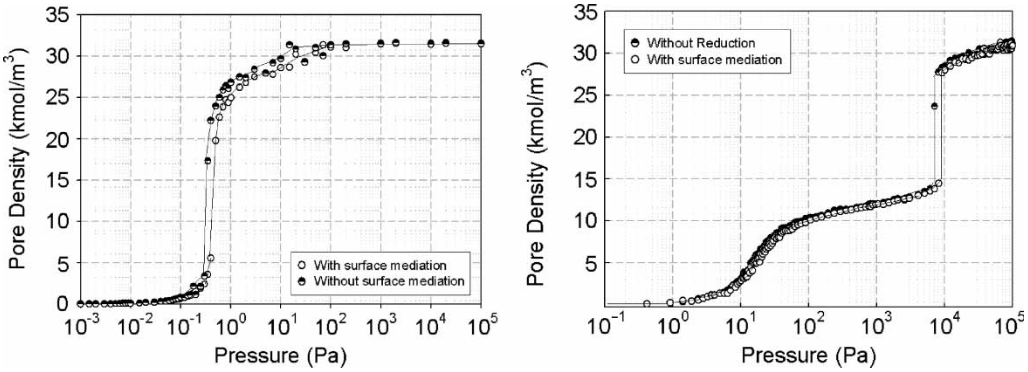

Figure 9. Adsorption isotherms in slit pore (half-filled symbol, no surface mediation; unfilled symbol, with surface mediation); (a) 10 A pore; (b) 20 A pore.

we found that about 1% of their surface is covered with the functional group and the surface-mediated damping constant is 0.0075. With this information, the GCMC-simulated results describe well the experimental adsorption isotherm over a very wide range of pressure. The importance of the surface mediation is also illustrated with the adsorption of nitrogen in 10 and 20 A slit pores. The difference between the isotherm obtained for the case of no surface mediation and that for the case of with surface mediation is significant enough, and this can have an implication that if incorrect local isotherms are used in the pore characterization, unreliable pore size distribution might be resulted.

Acknowledgements

This work is supported by the Australian Research Council.

References

[1] W.L. Jorgensen, J.D. Madura, C.J. Swenson. Optimized intermolecular potential functions for liquid hydrocarbons. *J. Am. Chem. Soc.*, **106**, 6638 (1984).

[2] C.S. Murthy, S.F. O-Shea, I.R. McDonald. Electrostatic interactions in molecular crystals. Lattice dynamics of solid nitrogen and carbon dioxide. *Mol. Phys.*, **50**, 531 (1983).

[3] D.D. Do, H.D. Do, K. Kaneko. Effect of a surface-perturbed intermolecular interaction on adsorption of simple gases on a graphitized carbon surface. *Langmuir*, **20**, 7623 (2004).

[4] M. Kruk, Z. Li, M. Jaroniec, W.R. Betz. Nitrogen adsorption study of surface properties of graphitized carbon blacks. *Langmuir*, **15**, 1435 (1999).

[5] S. Brunauer, P. Emmett, E. Teller. Adsorption of gases in multimolecular layers. *J. Am. Chem. Soc.*, **60**, 309 (1938).

[6] E.P. Barrett, L. Joyner, P. Halenda. The determination of pore volume and area distributions in porous substances. I. Computations from nitrogen isotherms. *J. Am. Chem. Soc.*, **73**, 373 (1951).

[7] K. Hovarth. Method for the calculation of the effective pore size distribution in molecular sieving carbon. *J. Chem. Eng. Japan* (1981).

[8] D.J. Adams. Grand canonical ensemble Monte Carlo for a Lennard-Jones fluid. *Mol. Phys.*, **29**, 307 (1975).

[9] G.E. Norman, Filinov. Investigation of phase transitions by a Monte Carlo method High Temperature (USSR), **7**, 216–222 (1969).

[10] W.A. Steele. Computer simulations of the structural and thermodynamic properties of adsorbed phases. Surfactant Science Series, 78 (Surfaces of Nanoparticles and Porous Materials) 319–354 (1999).

[11] W.A. Steele. Computer simulations of physical adsorption: A historical review. *Appl. Surface Sci.*, **196**, 3 (2002).

[12] J. Pikunic, C.M. Lastoskie, K.E. Gubbins. Molecular modeling of adsorption from the gas phase. *Handbook of Porous Solids*, **1**, 182 (2002).

[13] O. Sinanoglu, K.S. Pitzer. Interactions between molecules adsorbed on a surface. *J. Chem. Phys.*, **32**, 1279 (1960).

[14] D.H. Everett. Interactions between adsorbed molecules. *Disc. Farad. Soc.*, **40**, 177 (1965).

[15] A.D. McLachlan. Van der Waals forces between an atom and a surface. *Mol. Phys.*, **7**, 381 (1964).

[16] N.R. Laine, F. Vastola, P. Walker. The importance of active surface area in the carbon-oxygen reaction. *J. Phys. Chem.*, **67**, 2030 (1963).

[17] E. Brodskaya, E. Piotrovskaya. Computer modeling of nitrogen adsorption in micropores. *Russ. J. Phys. Chem.*, **75**, 623 (2001a).

[18] E. Brodskaya, E. Piotrovskaya. Monte Carlo modeling of the effect of changeover from micropores to mesopores for the adsorption of nitrogen adsorption in graphite micropores. *Russ. J. Phys. Chem.*, **75**, 1691 (2001b).

[19] E. Bottani, V. Bakaev. The grand canonical ensemble Monte Carlo simulation of nitrogen on graphite. *Langmuir*, **10**, 1550 (1994).

[20] R.F. Cracknell, D. Nicholson, S. Tennison, J. Bromhead. Adsorption and selectivity of carbon dioxide with methane and nitrogen in slit-shaped carbonaceous micropores: Simulation and experiment. *Adsorption*, **2**, 193 (1996).

[21] J. Potoff, I. Siepmann. Vapor-liquid equilibria of mixtures containing alkanes, carbon dioxide and nitrogen. *AIChE J.*, **47**, 1676 (2001).

[22] D. Frenkel, B. Smit. *Understanding Molecular Simulation*, Academic Press, New York (2002).

[23] P.A. Tipler. *Physics*, Freeman and Company/Worth Publishers, New York (1999).

[24] D. Heyes, F. van Swol. The electrostatic potential and field in the surface region of lamina and semi-infinite point charge lattices. *J. Chem. Phys.*, **75**, 5051 (1981).

[25] M. Maddox, J. Olivier, K. Gubbins. Characterization of MCM-41 using molecular simulation: Heterogeneity effects. *Langmuir*, **13**, 1737 (1997).

[26] A. Neimark, A. Vishnyakov. Gauge cell method for simulation studies of phase transitions in confined systems. *Phys. Rev. B*, **62**, 4611 (2000).

[27] W.A. Steele. Physical interaction of gases with crystalline solids. I. Gas-solid energies and properties of isolated adsorbed atoms. *Surface Sci.*, **36**, 317 (1973).

[28] W.A. Steele. International Encyclopedia of Physical Chemistry and Chemical Physics, Topic 14, Vol. 3: The Interaction of Gases with Solid Surfaces (1974).

[29] H.Y. Kim, W.A. Steele. Computer simulation study of the phase diagram of the CH_4 monolayer on graphite: Corrugation effects. *Phys. Rev. B*, **45**, 6226 (1992).

[30] D. Nicholson, N.G. Parsonage. *Computer Simulation and the Statistical Mechanics of Adsorption*, Academic Press, London (1982).

[31] P. Pascual, P. Ungerer, B. Tavitian, P. Pernot, A. Boutin. Development of a transferable guest-host force field for adsorption of hydrocarbons in zeolites. *Phys. Chem. Chem. Phys.*, **5**, 3684–3693 (2003).

[32] A.V. Klochko, E. Brodskaya, E. Piotrovskaya. Computer simulations of dependence of adsorption characteristics of ethane on the size of graphite micropores. *Langmuir*, **15**, 545 (1999).

[33] A.A. Isirikyan, A.V. Kiselev. The absolute adsorption isotherms of vapors of nitrogen, benzene and n-hexane, and the heats of adsorption of benzene and n-hexane on graphitized carbon blacks. *J. Phys. Chem.*, **65**, 601 (1961).

[34] S. Ross, W. Winkler. Physical adsorption. VIII. Monolayer adsorption of argon and nitrogen on graphitized carbon. *J. Coll. Sci.*, **10**, 319 (1955).

[35] D. Graham. Geometric heterogeneity in the adsorption of nitrogen on graphitized carbon surfaces. *J. Phys. Chem.*, **61**, 1310 (1957).

[36] R.A. Beebe, J. Biscoe, W. Smith, C. Wendell. Heats of adsorption on carbon black. *J. Am. Chem. Soc.*, **69**, 95 (1947).

[37] L. Joyner, P. Emmett. Differential heats of adsorption of nitrogen on carbon blacks. *J. Am. Chem. Soc.*, **70**, 2353 (1948).

[38] E. Pace, A. Siebert. Heats of adsorption and adsorption isotherms for low boiling gases adsorbed on graphon. *J. Phys. Chem.*, **64**, 961 (1960).

[39] J. Piper, J. Morrison, C. Peters, Y. Ozaki. Heats and entropies of adsorption of N_2 on grapfoil at 79.3 KJ. *J. Chem. Soc. Farad. Trans. I.*, **79**, 2863 (1983).